Sawtooth Instability and Magnetic Reconnection in Tokamak Plasma

P.V.Savrukhin, S.V. Tsaun

Russian Research Center "Kurchatov Institute", 123182, Moscow, Russia

e-mail contact of main author: psavruk@nfi.kiae.ru

Abstract. Bursts of the non-thermal x-ray spikes (E_γ~25-100keV) around X-point of the m=1,n=1 magnetic island are observed during a sawtooth crash in experiments in T-10 tokamak (R=1.5m, a=0.3m). Analysis indicated that the spikes can be connected with the non-thermal electrons generated during reconnection of the magnetic field lines around the q=1 surface. Results of the experimental studies are compared with modeling of generation of the non-thermal electron beams in strong electric fields. Analysis indicted that while the density of the non-thermal beams induced during the reconnection is two order of magnitude smaller that one of the background plasma, the beams can change magnetic shear around the q=1 surface and modify dynamic of the sawtooth crash.

1. Magnetic reconnection and non-thermal electrons in tokamak plasma

Plasma instability called “sawtooth oscillations” is one of the commonly observed phenomena in experiments in tokamaks [1]. The sawtooth instability is generally associated with growth of the large-scale magnetohydrodynamic (MHD) perturbations described by the theory of reconnection of the magnetic field lines around the $q=1$ magnetic surface (here, $q=d\psi_t/d\psi_p$, ψ_t, ψ_p - toroidal and poloidal magnetic fluxes, accordingly) [2]. Magnetic reconnection is a complicated process of plasma flows and rearrangement of the magnetic field lines appeared inside a narrow region (reconnection layer) where topologically different magnetic flux tubes met each other (see [3]). Inside the reconnection layer various dissipative and non-linear effects (such as finite resistivity, viscosity, and inertia, as well as magnetic turbulence) can lead to effective decoupling of the plasma flows from the magnetic fields. Diffusion of the magnetic fluxes leads to interconnection of the field lines inside the reconnection layer with subsequent release of the magnetic energy and its transformation into radiation, plasma heating, and particles acceleration.

Importance of the particle acceleration during the reconnection process was realized initially in analysis of the Astrophysics phenomena, such as Solar flares and processes in the Earth magnetosphere [4]. The problem was considering theoretically as early as in 1966 in paper by Syrovatskii [5]. Theoretical analysis as well as measurements in laboratory experiments [6] has indicated that fast changes of the magnetic fields during the impulsive phase of the reconnection can lead to generation of the electric field up to E~300V/m and subsequent production of the high-energy electrons. Particle acceleration during the reconnection can be also provided due to the shock waves [7], plasma turbulence (see [3]), and whistler waves [8].

Acceleration of the electrons during the reconnection process is equally important in tokamak plasma [3,9-11]. Extensive theoretical studies made so far have identified physics basis of runaway formation, loss and wall interaction in both present and reactor-scale tokamaks (see review [12]). While details of the process are still arguing in the literature, it is generally accepted that the non-thermal electrons are produced mainly due to Dreicer acceleration (primarily mechanism) [13] and knock-on avalanches [14]. Both mechanisms depend critically on amplitude of the longitudinal electric field E (see Fig.1), which (at the quasi-stationary stage of the discharge) is specified by the inductive equilibrium electric field E_0. Moreover, it is generally accepted that presence of the MHD modes facilitates loss of the pre-

existent runaway electrons due to the enhanced diffusion in the turbulent magnetic fields (see, [15-18]). It is speculated, however, that the non-thermal electrons can be produced due to strong electric fields ($E>E_c$, E_c – critical Dreicer field, see below) induced during the reconnection of the magnetic field around the resonant surfaces. Simplified modeling indicated that while the total number of the suprathermal electrons involved in the process is small they can substitute considerable fraction of the plasma current (comparable with the inductive current inside the *q=1* area). Suprathermal electrons in the case can provide strong modification of dynamic of the tearing mode and should be analyzed in details in the experiments. Present paper represents results of the experimental studies of the non-thermal electrons induced during sawteeth instability in T-10 tokamak (see Section 2). Possible mechanisms of generation and loss of the suprathermal electrons, as well as results of the numerical simulations are considered in Section 3.

2. Non-thermal x-ray bursts during sawtooth crash in T-10 plasma

Experiments in T-10 indicated that sawteeth crashes in high density plasma ($<n_e>$ up to 4.5 $10^{19}m^{-3}$) are typically accompanied by intensive bursts of the non-thermal x-ray radiation [11]. Measurements using *Si* and *CdTe* detectors placed at various angular position around the torus (see [19,20]) have indicated that the burst are spatially localized around the X-points of the *m=1,n=1* magnetic island. The x-ray bursts during a sawtooth crash are observed most clearly with the tangentially viewing x-ray detector, while they are also detected with the conventional x-ray tomographic arrays. During a sawtooth crash, the x-ray bursts appear initially around the sawtooth inversion surface and are later displaced to the outer radii at the top of the heat pulse propagating through the plasma (Fig.2). Amplitude of the x-ray bursts decreases monotonically as they propagate to the outer radii. It should be noted, that normal heat pulses induced during the sawtooth crash outside the *q=1* surface decay at considerably slower rate in comparison with the x-ray bursts disappearing in a fraction of millisecond ($\delta t<0.1ms$). During sawtooth crash the x-ray bursts are observed consecutively along various chords across the plasma cross-section simultaneously with maximum perturbation due to the rotated m=1 mode. In subsequent sawtooth crashes x-ray bursts can be initiated in various angular position (either at high or low field side of the torus) depending on position of the *m=1,n=1* mode (Fig.2).

In contrast with the “classical” hard x-ray bursts, generally observed during major disruptions [21], the “internal” x-ray spikes observed during a sawtooth crash are not accompanied by the enhanced radiation from the plasma limiters. This observation seems can exclude possible role of the plasma-wall interaction in generation of the non-thermal emission during a sawtooth crash. Moreover, observation of the x-ray spikes at any position along the poloidal circumference (including high-field side of the torus) seems also excludes possible ballooning origin of the spike-like perturbations (see [22]).

3. Generation of the non-thermal electrons during a sawtooth crash

Observation of the x-ray spikes during abrupt growth of the *m=1,n=1* perturbations can possibly indicate connection of the phenomena with the magnetic reconnection. Schematic view of generation of the non-thermal electrons during sawtooth crash is shown in Fig.3. Growth of the m=1,n=1 mode (solid displacement of the plasma core) during the crash leads to squeezing and reconnection of the magnetic field lines with different pitch angles around the q=1 surface. Amplitude of the induced electric field can be determined in the case by rate of change of the perturbed helical magnetic field B^* inside current layer with width δ_{rec}

around the q=1 surface: $E_1 = -\delta_{rec}\, dB^*/dt$. The perturbed field, $B^*=B_p-(r/R)B_t$, is calculated for parabolic current density profile with specified displacement of the plasma core $\xi_1(t)$: $\xi_1 \sim r_1[1-\exp(-\gamma_1 \Delta t)]^{\alpha 1}$. Here, $\gamma_1=(s_1 a^2/(r_1 R))^{2/3}(\tau_R/\tau_A)^{2/3}/\tau_R$ is increment of the m=1 mode [23], s_1 - magnetic shear around the resonant surface $r=r_1$, τ_R, τ_A -magnetohydrodynamic and magnetic diffusion time scales, accordingly, and constants ξ_0, α_1 are chosen to fit the experimentally observed time scale of the sawtooth crash ($\alpha_1 \sim 2$ for $\Delta t_{crash} \sim 100\mu$sec). Induced electric field ($E_1 > E_c$) provides generation of the non-thermal electron beams with density N_{r1} (see above). Simultaneous growth of the magnetic field perturbations (δB_1) can remove the non-thermal electrons from the reconnection layer to the larger radii ($r > r_1$) and effectively limit the density of the beams. The non-thermal beams propagate through the plasma cross-section and are accompanied by bursts of the non-thermal x-ray emission with delay at the outer radii.

In a simplified way the generation of the non-thermal electrons in plasma with longitudinal electric field (E) can be described by equation: $dN_r/dt = n_e/\tau_{dr} + N_r/\tau_{av} - \nabla\, \Gamma_{loss}$, where N_r , n_e- density of the non-thermal electrons and background plasma, $1/\tau_{dr}$ and $1/\tau_{av}$ represent production rates of the primary non-thermal electrons (Dreicer acceleration) [13] and the secondary knock-on avalanche [14], accordingly, flux Γ_{loss} denotes losses of the non-thermal electrons. Primary production of the non-thermal electrons in intrinsically thermal plasma is mainly determined by balance of the particle acceleration in the electric field and scattering due to Column collisions. Production rate of the primary electrons is described by relation (see [12]): $\tau_{dr}^{-1} \approx 0.3\, \nu_e\, \varepsilon_d^{-3(Zeff+1)/16} \exp(-1/4\varepsilon_d - ([Z_{eff}+1]/\varepsilon_d)^{1/2})$, where $\varepsilon_d = E/E_c$, E_c is the critical (threshold) electric field given by $E_c = e^3 n_e Z_{eff} \ln\Lambda/(4\pi\varepsilon_0^2 m_e v_{th}^2)$, ν_e is the collision frequency of the electrons at the thermal velocity v_{th} and Z_{eff} is the effective plasma charge ($Z_{eff} \approx 1$). In plasma with seed population of the non-thermal electrons, the knock-on avalanche due to close collisions of the electrons determines production rate of the beams: $\tau_{av}^{-1} \approx 2 m_e c \ln\Lambda\, a(Z_{eff})/eE$, where $a(Z_{eff}=1) \approx 1$ [14,24]. It is established in previous studies that macro-scale magnetic turbulence constitutes the dominant loses of the non-thermal electrons during the disruption [15-18]. Such loses can be represented in a simplified way by the flux $|\Gamma_{loss}| = D_{rt}\, \partial N_r/\partial r$, where the diffusion coefficient D_{rt} is determined by the amplitude of magnetic field perturbations $\delta B/B_t$: $D_{rt} \approx (\pi R_0 q v_r)(\delta B/B_t)^2$, $|v_r| \sim 0.5c$ is the non-thermal electrons mean velocity. The magnetic field perturbations are represented by radial function decaying outside the resonant magnetic surface: $\delta B = (r_1/r)^{m+1}\, \delta B_1$.

Results of the simulations obtained with a typical set of parameters determined on the base of T-10 experimental data are shown in Fig.3b. Calculated growth rate of the electron beams ($\gamma_r \sim 10^4 s^{-1}$) and velocity of the beams propagation outside the q=1 surface ($V \sim 10^3 m/s$) agree with ones determined from analysis of the x-ray perturbations observed in the experiments. Calculations indicate that production rate and losses of the non-thermal beams depend critically on amplitude of the induced electric fields and magnetic field perturbations (see Fig.3d). Phenomena of generation of the non-thermal electrons is essential during abrupt growth of the MHD modes while it can be diminished in presence of the continuous MHD perturbations with saturated amplitude. This is also in qualitative agreement with the experiments in T-10. Density of the non-thermal electrons induced during sawtooth crash is up to two order of magnitude smaller than one of the background plasma. However, they can carry considerable fraction of the longitudinal plasma current (of order of $I_{RA} \sim 10\text{-}20\ kA$). Such currents (comparable with an equilibrium current inside the q=1 surface in T-10 plasma) can considerably change classical mechanisms of the sawtooth instability typically considered in the theory.

It should be pointed out that while effect of the electron acceleration during a sawtooth crash is well established in the experiments, no consensus is reached so far about mechanisms of the phenomena. Situation is complicated by necessity of analysis of plasma dynamic inside narrow current layer determined by such physical processes as resistive diffusion, electron viscosity and inertia, as well as magnetic turbulence and shock waves not measured directly in experiments in tokamaks. Width of reconnection layer is calculated in present simulations using simplified relation [9]: $\delta_{rec}^2 = \alpha_2 \left[(\tau_A/\tau_R) r_1^2 + (c/\omega_p)^2 \right]$, where two terms in square brackets represent effects of magnetic diffusivity and electron inertia accordingly and parameter α_2 $(\alpha_2 \sim 1)$ represents other possible dissipative effects (here, $\omega_p^2 = ne^2/\varepsilon_0 m$ – electron plasma frequency). Such oversimplified treatment of the reconnection layer can be used for general description of the non-thermal beams formation and loss during growth of the MHD modes, while numerical calculations using 3D MHD and kinetic simulations (see [22, 25-27]) are required for analysis of the phenomena. Moreover, in spite of considerable progress made in resent years in analysis of the internal magnetic fields in tokamak plasma, accuracy of the measurements is still not high enough for unambiguous study of temporal evolution of the magnetic fluxes inside narrow current layer during the reconnection. Experimental measurements of the plasma parameters around the reconnection layer are still restricted to laboratory experiments (see for example [28]). Measurements of the magnetic fields inside the reconnection layer is one of the primarily task of future experimental studies of the sawteeth in tokamaks.

In conclusion, analysis of the experiments in T-10 tokamak indicated that the non-thermal x-ray bursts observed during a sawtooth crash can be connected with suprathermal ($E_\gamma \sim 25\text{-}100$ *keV*) electron beams induced during magnetic reconnection around X-point of the m=1,n=1 magnetic island. Production rate and losses of the non-thermal beams depend critically on amplitude of the induced electric field and magnetic field perturbations.

The work is supported by Nuclear Science and Technology Department of Minatom RF and Russian Fund for Basic Research, Grant 01-02-16768.

References

1 S. VonGoeler, et al., Phys. Rev. Lett., **33** (1974) 1201.
2. B. B. Kadomtsev, Sov. J. Plasma Phys., **1** (1975) 389.
3. D. Biskamp, *Magnetic reconnection in plasmas*, Cambridge University Press, Cambridge, 2000.
4. E. R. Priest, *Solar Magnetohydrodynamic* (Reidel, Dordrecht, 1984).
5. S. I. Syrovatskii, Astron. Zh. (Sov. Astron.) **43**, (1966) 340.
6. N. P. Kyrie, et al., Fizika plazmi, **3** (1977) 538.
7. C. DeJager, Solar Phys., **64** (1980) 135.
8. J. F. Drake, Nature (London) **410** (2001) 525
9. J. A. Wesson, Nucl. Fusion, **30** (1990) 2545.
10. M. Erba, et al., Nucl. Fusion, **33** (1993) 1577.
11. P. V. Savrukhin, Phys. Rev. Lett., **86** (2001) 3036.
12. ITER Physics Expert Group, ITER Physics Basis Editors, Nucl. Fusion, **39** (1999) 2251.
13. H. Dreicer, Phys. Rev., **117** (1960) 329.
14. M. N. Rosenbluth, et al., Nucl.Fusion,**37**(1997)1355.
15. H. E. Mynick, et al., Phys. Fluids, **24** (1981) 695.
16. R. Yoshino, S. Tokuda, Nucl. Fusion,**40** (2000) 1293.
17. P. Helander, L.-G. Eriksson, F. Andersson, Phys. Plasmas, **7** (2000) 4106.
18. A. B. Rechester, et al., Phys.Rev.Lett.,**40**(1978)38.
19. P. V. Savrukhin, I. V. Klimanov, Rev. Sci. Instrum. **72** (2001) 1668.
20. P. V. Savrukhin, Rev. Sci. Instrum. **73** (2002),N12.
21 R. D. Gill, *et al.*, Nucl. Fusion, **40** (2000) 163.
22. W. Park, D. A. Monticello, E. D. Fredrickson, K. McGuire, Phys. Fluids, B **3** (1991) 507.
23. G. Bateman, *MHD Instability* (The MIT Press, Cambridge, 1979) 148.
24. R. Jaspers, et al., Nucl. Fusion, **36** (1996) 367.
25. A. M. Popov, et al., Bulletin of the American Physical Society **45**, 278 (2000).
26. B. N. Rogers, R. E. Denton, J. F. Drake, and M. A. Shay, Phys. Rev. Lett., **87** (2001) 195004.
27. Xiaogang Wang, A. Bhattacharjee, and Z.W. Ma, Phys. Rev. Lett. **87**, (2001) to be published.
28. M. Yamada, H. Ji, S. Hsu, T. Carter, R. Kulsrud, and F. Trintchouk, Phys. Plasmas, **7** (2000) 1781.

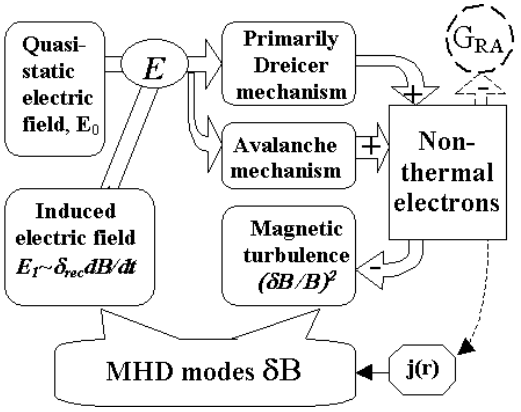

Fig.1. Schematic view of the mechanisms leading to generation of the non-thermal electron beams in a tokamak plasma.

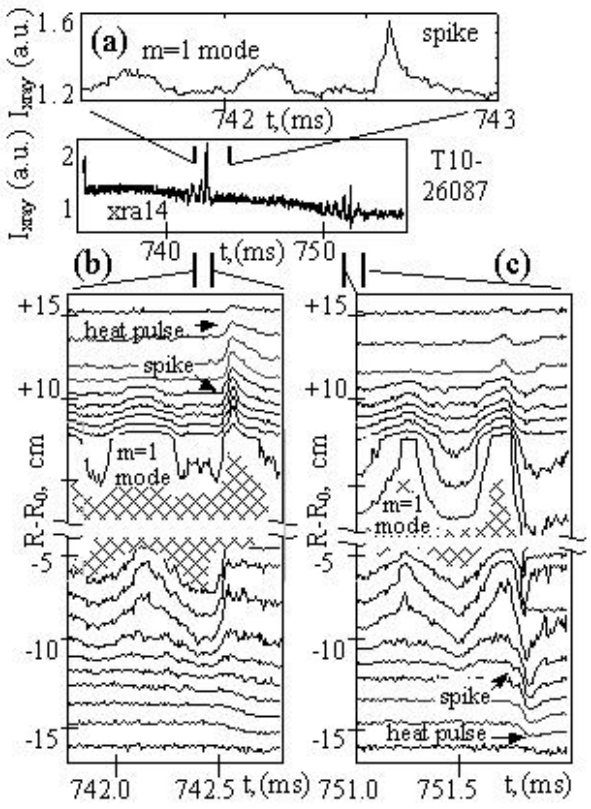

Fig.2. Time evolution of the x-ray intensity (a) and x-ray contour plots (b,c) measured using vertical x-ray array. The non-thermal spikes (superimposed with the m=1 mode) are observed at the low and the high field side of the torus during subsequent sawtooth crashes (see t~742.55ms and t~751.8ms in frames (b),(c), accordingly). Contour lines in the center ($|R-R_0| \leq 3$-5cm) are not shown in the figure due to high level of the x-ray intensity (see dashed area).

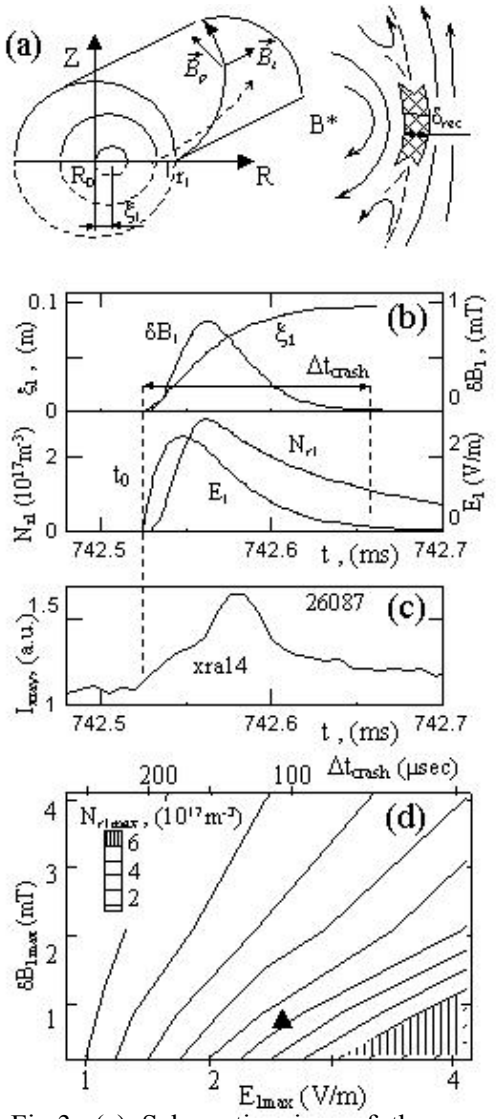

Fig.3. (a) Schematic view of the magnetic flux surfaces and perturbed helical magnetic field B^* during the sawtooth crash. Non thermal electrons are generated inside the current layer with width δ_1 formed during reconnection of the magnetic field B^* around the q=1 surface. (b) Time evolution of calculated density of the non-thermal electrons (N_{r1}) generated due to electric field (E_1) induced around the q=1 surface during radial displacement of the plasma core (ξ_1). Growth of the beams is limited due to the magnetic field perturbations (δB_1). (c) Time evolution of the x-ray intensity measured in experiments in T-10 along the vertical chord tangential to the q=1 surface Frame (d) represents contour plot of the maximum non-thermal electron density (N_{r1max}) calculated in plasma with various amplitude of the induced electric field (E_{1max}) and magnetic field perturbations (δB_{1max}).